Linkage Isomerization in $M(CO)_5(DHF)$ Complexes ($M =$ Cr, Mo, W; DHF = 2,3-Dihydrofuran, 2,5-Dihydrofuran) Studied by Time-Resolved Infrared Absorption Spectroscopy

A. Shagal and Richard H. Schultz*

Department of Chemistry, Bar-Ilan University, 52900 Ramat-Gan, Israel

Received February 1, 2002

Photolysis of a cyclohexane (CyH) solution of $M(CO)_6$ ($M =$ Cr, Mo, W) in the presence of excess 2,3- or 2,5-dihydrofuran (DHF) yields the complex $M(CO)_5(DHF)$. The solvated complex $M(CO)_5(CyH)$ formed upon photolysis reacts with DHF to form, with a second-order rate constant of 10^6-10^7 L mol^{-1} s^{-1}, a single product, identified as the O-bound complex $M(CO)_5(\eta^1\text{-DHF})$. On a longer time scale (milliseconds to seconds), equilibrium is established between this kinetic product and a second product, $M(CO)_5(\eta^2\text{-DHF})$, in which the ligand is bound to the metal through the DHF C=C double bond, via an intramolecular linkage isomerization reaction. Time-resolved infrared absorption spectroscopy (TRIR) is used to monitor the kinetics of this linkage isomerization, and activation and equilibrium parameters for the isomerization are determined. For all six systems, $\Delta H^{\ddagger} \approx 15$ kcal mol^{-1}, while the isomerization is thermoneutral or slightly exothermic ($|\Delta H°| \approx 0-2$ kcal mol^{-1}). Trends in reactivity as a function of the metal and of the ligand are discussed, and the utility of TRIR as a method for investigating intramolecular linkage isomerization in carbonyl complexes is assessed.

Introduction

In a previous communication from this laboratory,[1] we presented results of a study of the photochemical reaction of $W(CO)_6$ with 2,5-dihydrofuran (2,5-DHF) in cyclohexane (CyH) solution. The immediate product of $W(CO)_6$ photolysis, $W(CO)_5(CyH)$,[2] undergoes a bimolecular reaction with DHF (second-order rate constant $\sim 10^7$ L mol^{-1} s^{-1}) to form a product to which we assigned the O-bound $W(CO)_5(\eta^1\text{-DHF})$ structure.[3] This assignment was based on the similarity of the product's IR spectrum to that of $W(CO)_5(THF)$ (Figure 1). On a time scale of seconds, however, the absorbances corresponding to $W(CO)_5(\eta^1\text{-DHF})$ disappear, while simultaneously, a new product appears. The first-order rate constant for this second reaction (~ 1 s^{-1}) is independent of [DHF] and of [$W(CO)_6$]. The identity of this product as the C,C-bound $W(CO)_5(\eta^2\text{-DHF})$ isomer was deduced from the similarity of its IR spectrum to those of known $W(CO)_5$(alkene) complexes; its structure was confirmed by ^{1}H NMR spectroscopy. We were able to follow the conversion of the η^1 isomer to the η^2 isomer (reaction 1) by time-resolved IR absorption spectroscopy (TRIR). As can be seen in Figure 1, the reaction in this case proceeds nearly to completion.

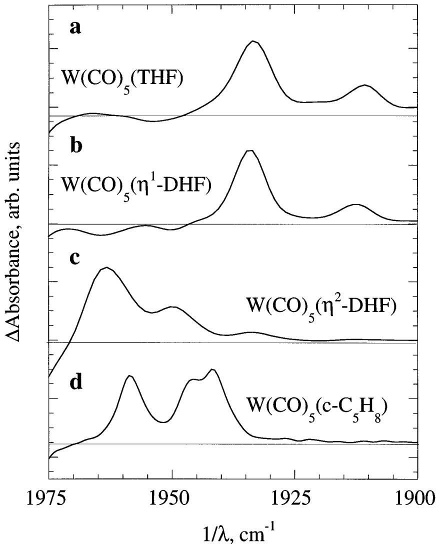

Figure 1. Room-temperature IR absorption spectra (1900−2000 cm^{-1}) of some $W(CO)_5L$ complexes in CyH solution: (a) spectrum of $W(CO)_5(THF)$; (b) spectrum of $W(CO)_5$(2,5-DHF) obtained 25 μs after photolysis of a solution containing $W(CO)_6$ (0.5 mmol L^{-1}) and 2,5-DHF (0.15 mol L^{-1}); (c) spectrum of $W(CO)_5$(2,5-DHF) obtained several minutes after 308 nm photolysis (∼300 laser shots) of a solution containing $W(CO)_6$ and excess 2,5-DHF; (d) spectrum of $W(CO)_5$(cyclopentene).

$$M(CO)_5(\eta^1\text{-DHF}) \rightarrow M(CO)_5(\eta^2\text{-DHF}) \qquad (1)$$

---

* To whom all correspondence should be addressed. Email: schultr@mail.biu.ac.il. Fax: +972-3-535-1250.

(1) Elgamiel, R.; Huppert, I.; Lancry, E.; Yerucham, Y.; Schultz, R. H. *Organometallics* **2000**, *19*, 2237.

(2) (a) Welch, J. A.; Peters, K. S.; Vaida, V. *J. Phys. Chem.* **1982**, *86*, 1941. (b) Simon, J.; Peters, K. S. *Chem. Phys. Lett.* **1983**, *98*, 53. (c) Wang, L.; Zhu, X.; Spears, K. G. *J. Am. Chem. Soc.* **1988**, *110*, 8695. (d) Lee, M.; Harris, C. B. *J. Am. Chem. Soc.* **1989**, *111*, 8963. (e) Xie, X.; Simon, J. D. *J. Phys. Chem.* **1989**, *93*, 4401. (f) Joly, A. G.; Nelson, K. A. *Chem. Phys.* **1991**, *152*, 69.

(3) Lugovskoy, A.; Paur-Afshari, R.; Schultz, R. H. *J. Phys. Chem. A* **2000**, *104*, 10587.

10.1021/om020084f CCC: $22.00

Two complexes that differ only in the geometry of ligand binding by an ambidentate ligand are known as *linkage isomers*. While the first example of a complex that undergoes linkage isomerization, $Co(NH_3)_5(NO_2)^{2+}$, was reported in 1857,[4] the second example was not characterized until more than a century later.[5] In the ensuing 40 years, linkage isomerization has been extensively studied,[6] the majority of the research having been on linkage isomerization of inorganic ligands such as SCN^- and NO_2^-. Isomerizations analogous to the one we observed for $W(CO)_5(DHF)$, in which an organic ligand undergoes a $\eta^1(\sigma) \rightarrow \eta^2(\pi)$ hapticity shift, have been observed for a variety of systems such as a series of [Os]−amine complexes containing aniline ligands,[6h] Pd(II)-chloranilate complexes,[7] a series of [Re]−aldehyde complexes,[8] complexes containing thiophene and related ligands,[9] and $Cr(CO)_5$(5-chloropentene).[10] While kinetic studies of the mechanisms of linkage isomerization[6c,h,j,10,11] date back to the 1950s, most of the research thus far performed on linkage isomerization has emphasized the properties of equilibrium mixtures of the linkage isomers rather than directly probing the dynamics of the process that connects them. In most cases, either one isomer is so much less stable than the other that it does not live long enough to be detected, or the approach to equilibrium is more rapid than the mixing time.

"Fast" time-resolved spectroscopy is an ideal method for investigation of the kinetics of linkage isomerization. In most cases, the spectra (vibrational or electronic) differ significantly between the two isomers;[1,5] therefore, it is possible to measure the reaction kinetics by observation of the time-dependent changes in the reaction solution's spectrum. Because "fast" (time resolution <1 μs) kinetic methods were developed as a means of observing unstable transient species, they can be used to monitor both the kinetics of the initial formation of the complex and any subsequent isomerization and thus measure both the kinetics and the thermodynamics of the isomerization.

Not only is "fast kinetics" ideal for studying linkage isomerization, but linkage isomerization is an ideal subject for fast kinetic study. One general motivation for studying transient organometallic complexes is that they are good models for the coordinatively unsaturated unstable species that are frequently invoked as intermediates in catalytic processes. Since the first interaction between such an intermediate and its substrate is the binding of the substrate to the active site, understanding the reactions of the transient species that are the subject of fast kinetic studies can give us a deeper insight into the requirements for optimizing the catalyst−substrate interaction. In this sense, we can consider binding of a ligand to a transition-metal intermediate followed by linkage isomerization as a model for the geometrical preferences (kinetic and thermodynamic) for catalyst−substrate bonding.

The present study was undertaken in an effort to extend in two directions the results discussed in our preliminary communication. First, we wanted to know if the process observed for reaction of W with DHF (initial η^1 binding followed by unimolecular isomerization) also occurs with Cr and Mo. We further hoped to determine what trends (if any) might appear and how the linkage isomerization process compares to the well-studied ligand exchange reactions of these metals. In addition, the present report extends the initial study to include reactions of 2,3-DHF. We had previously observed that the kinetics of formation of $W(CO)_5(\eta^1$-2,3-DHF) displayed some anomalies relative to reactions of other five-membered O-containing heterocycles[3] and were therefore curious to know how the kinetics and thermodynamics of reaction 1 would be affected by the differences between the two isomers of DHF.

Experimental Section

The TRIR apparatus on which these experiments were performed has been described in detail elsewhere.[12] Briefly, reaction takes place in a temperature-controlled 0.5 mm path length IR cell. In most of the experiments discussed here, the temperature was within ±0.2 °C of the nominal reaction temperature; for reactions taking place at temperatures >50 °C or <15 °C, the temperature control was less exact, but in all cases, the cell temperature remained within ±0.5 °C of the nominal temperature during the course of the measurement. Reaction is initiated by the pulsed output of a XeCl excimer laser (308 nm, pulse width ∼20 ns, typically 30−80 mJ/pulse) of a CyH solution containing $M(CO)_6$ (M = Cr, Mo, W; typically $\sim 5 \times 10^{-4}$ mol L^{-1}) and excess DHF (0.02−3 mol L^{-1}). The photolysis causes, within the laser flash,[2] loss of a carbonyl ligand and solvation of the resulting "naked" pentacarbonyl to $M(CO)_5(CyH)$. The reaction solution flows through the cell so that each photolysis pulse irradiates fresh solution.

The progress of the reaction is monitored by measuring the time dependence of the IR absorption of the solution following the laser flash, using one of two independent IR sources. For kinetic experiments, we use a continuously tunable CW Pb-salt diode laser that has been set to a wavelength corresponding to an absorbance of the reaction intermediate or of the product, and the time dependence of the changes in IR signal reaching the detector (MCT, rise time ∼20 ns) measured. For measurement of time-dependent spectra, in particular, for determination of the locations of the IR absorptions of the species of interest, we use a Bruker Step-Scan FTIR (S^2FTIR) spectrometer. For any particular reaction, first-order or pseudo-first-order rate constants are determined by a least-squares linear fit to $\ln |A_0 - A_\infty|$.

---

[4] (a) Gibbs, W.; Genth, F. A. *Am. J. Sci.* **1857**, *24*, 86. (b) Werner, A. *Ber. Dtsch. Chem. Ges.* **1907**, *40*, 765.

[5] Basolo, F.; Hammaker, G. S. *Inorg. Chem.* **1962**, *1*, 1.

[6] (a) Fraser, R. T. M. *Adv. Chem. Ser.* **1967**, *No. 62*, 295. (b) Burmeister, J. L. *Coord. Chem. Rev.* **1968**, *3*, 225. (c) Jacobson, S. E.; Reich-Rohrwig, P.; Wojcicki, A. *Inorg. Chem.* **1973**, *12*, 717. (d) Balahura, R. J.; Lewis, N. A. *Coord. Chem. Rev.* **1976**, *20*, 109. (e) Jackson, W. G.; Sargeson, A. M. In *Rearrangements in Ground and Excited States*; de Mayo, P., Ed.; Academic Press: New York, 1980; Vol. 2, p 336. (f) Orell, K. G. *Mech. Inorg. Organomet. React.* **1989**, *6*, 337. (g) Burmeister, J. L. *Coord. Chem. Rev.* **1990**, *105*, 77. (h) Taube, H. *Pure Appl. Chem.* **1991**, *63*, 651. (i) Buckingham, D. A. *Coord. Chem. Rev.* **1994**, *135/136*, 587. (j) Keiter, R. L.; Benson, J. W.; Keiter, E. A.; Lin, W.; Jia, Z.; Olson, D. M.; Brandt, D. E.; Wheeler, J. E. *Organometallics* **1998**, *17*, 4291. (k) Cole, S.; Dulaney, K. E.; Bengali, A. A. *J. Organomet. Chem.* **1998**, *560*, 55. (l) Gibney, S. C.; Ferraudi, G.; Shang, M. *Inorg. Chem.* **1999**, *38*, 2898. (m) Cronin, L.; Higgitt, C. L.; Perutz, R. N. *Organometallics* **2000**, *19*, 672.

[7] Jeong, W.-Y.; Holwerda, R. A. *Inorg. Chem.* **1988**, *27*, 2571.

[8] Quirós Méndez, N.; Seyler, J. W.; Arif, A. M.; Gladysz, J. A. *J. Am. Chem. Soc.* **1993**, *115*, 2323.

[9] Recent reviews: (a) Chen, J.; Angelici, R. J. *Coord. Chem. Rev.* **2000**, *206−207*, 63. (b) Angelici, R. J. *Organometallics* **2001**, *20*, 1259.

[10] Ladogana, S.; Nayak, S. K.; Smit, J. P.; Dobson, G. R. *Inorg. Chem.* **1997**, *36*, 650.

[11] (a) Basolo, F.; Stone, B. D.; Bergmann, J. G.; Pearson, R. G. *J. Am. Chem. Soc.* **1954**, *76*, 3079. (b) Pearson, R. G.; Henry, P. M.; Bergmann, J. G.; Basolo, F. *J. Am. Chem. Soc.* **1954**, *76*, 5920.

[12] Paur-Afshari, R.; Lin, J.; Schultz, R. H. *Organometallics* **2000**, *19*, 1682.

Table 1. C−O Stretching Frequencies (cm^{-1}) and Force Constants[a] (10^2 N m^{-1}) for $M(CO)_5(CyH)$ and $M(CO)_5(DHF)$ Complexes

					$M(CO)_5(\eta^1\text{-DHF})$						$M(CO)_5(\eta^2\text{-DHF})$					
	$M(CO)_5(CyH)$			DHF isomer	ν_{CO}			force constant			ν_{CO}			force constant		
M	$A_1(1)$	E	$A_1(2)$		$A_1(1)$	E	$A_1(2)$	k_t	k_c	k_i	$A_1(1)$	E	$A_1(2)$	k_t	k_c	k_i
Cr	2083	1957	1933	2,5	2071	1940	1913	14.995	15.840	0.318	2081	1964	1959	15.693	16.155	0.287
				2,3	2075	1943	1915	15.028	15.893	0.321	2069	1954	1945	15.468	15.984	0.280
Mo	2088	1964	1929	2,5	2077	1945	1914	15.013	15.925	0.322	2082	1966	1952	15.581	16.183	0.285
				2,3	2077	1947	1916	15.041	15.947	0.317	2077	1961	1941	15.408	16.102	0.284
W	2087	1954	1928	2,5[b]	2077	1936	1914	15.027	15.826	0.343	2083	1963	1952	15.588	16.154	0.294
				2,3	2075	1934	1913	15.011	15.794	0.343	2077	1957	1940	15.399	16.058	0.293

Legend: k_t, C−O trans to DHF; k_c, C−O cis to DHF; k_i, interaction force constant for mutually cis carbonyls. [a] Force constants were calculated using the Cotton−Kraihanzel method (Cotton, F. A.; Kraihanzel, C. S. *J. Am. Chem. Soc.* **1962**, *84*, 4432). [b] Reference 1.

In our initial measurements of the kinetics of the reaction on relatively long time scales (>10 ms), we observed that the time dependence of the absorption changes was not single exponential, despite the experimental conditions which should lead to a simple exponential time dependence whether the reaction is bimolecular or intramolecular. On further investigation, we discovered that for reactions that do not go to completion within ∼10 ms, the flow of the reaction solution through the cell carries the photolyzed sample out of, and unphotolyzed solution into, the path of the IR beam before the reaction is complete. Therefore, for the experiments in which the reaction required more than 0.5 ms to go to completion, the reactant flow was shut off during the measurement of the time-dependent IR spectrum and fresh solution supplied to the cell only during the interval between successive laser flashes. To ensure that there would be no complications from instrumental AC time constants on the measurement of the time dependences of the IR absorptions, all experiments were done with the detector and digital oscilloscope DC coupled. Placing a 15 μF capacitor in series with the signal did not affect the observed time dependences, implying that we were observing the actual kinetic behavior of the system rather than a system AC time constant.[13]

Experiments were performed using HPLC grade CyH (99.8%, Lab-Scan Analytical Sciences) distilled from Na/benzophenone immediately prior to use. DHF is obtained from commercial sources (purity of >97% confirmed by NMR) and used as received except for distillation from an appropriate drying agent.

Results

General Remarks. The general course of the reaction is essentially the same for all six systems (M = Cr, Mo, W; DHF = 2,3-DHF, 2,5-DHF) studied here. Within the system rise time, absorbances corresponding to the C−O stretches of $M(CO)_5(CyH)$[12,14] appear. These absorbances disappear with time, while simultaneously, new peaks appear in the C−O stretching region of the IR spectrum. The rate at which these spectral changes occur depends on the particular metal and DHF isomer, as well as [DHF]; in all cases studied here, the experimental conditions were such that they occur over the course of 5−50 μs. We attribute the product peaks to C−O stretches of the O-bound complex $M(CO)_5(\eta^1\text{-DHF})$.[1,3] On a longer time scale (milliseconds to seconds), the absorbances that had appeared within microseconds decay, while simultaneously, a third set of IR absorbances, corresponding to a second reaction product, appear. We attribute these new C−O stretches to the C,C-bound isomer $M(CO)_5(\eta^2\text{-DHF})$. The observed values of the C−O stretches are summarized in Table 1 for both isomers of the six $M(CO)_5(DHF)$ complexes of the group 6 metals. In all cases, the C−O stretches of the second product have significantly higher frequencies than those of the initial product, consistent with our structural assignments. We have previously presented results for the formation of $W(CO)_5(\eta^1\text{-DHF})$ from the reaction of $W(CO)_5(CyH)$ with 2,5-DHF and 2,3-DHF.[3] Since in the present experiment we were concerned only with the isomerization reaction that produces the η^2-bound complex, no detailed kinetic studies of the initial reaction to form $M(CO)_5(\eta^1\text{-DHF})$ were performed for Cr or Mo.

For all of the systems investigated in the present study, pseudo-first-order rate constants for reaction 1 were determined from the time dependence of the decay of the low-frequency A_1 C−O stretch of the η^1 isomer (∼1915 cm^{-1}, Table 1). Rate constants determined from the rise of absorptions corresponding to the η^2 isomer were the same to within experimental error for a given reactant and temperature. Our choice of the ∼1915 cm^{-1} band as the kinetic probe was motivated primarily because, as described below, the absorbance of that band can be used to derive information about the relative amounts of the two isomers present in the solution.

$W(CO)_5(DHF)$. The linkage isomerization of $W(CO)_5(\eta^1\text{-2,5-DHF})$ has been discussed in our previous communication.[1] Briefly, over the temperature range 20−60 °C, the experimentally observed first-order rate constant for reaction 1 (k_{obs}) varies from ∼1 to ∼50 s^{-1}. At any given temperature, this rate constant is independent of the initial concentrations of $W(CO)_6$ and 2,5-DHF. The independence of k_{obs} from $[W(CO)_6]$ or [DHF] indicates that the formation of $W(CO)_5(\eta^2\text{-2,5-DHF})$ is unimolecular (reaction 1) rather than via ligand exchange from free DHF or from a second molecule of $W(CO)_5(\eta^1\text{-2,5-DHF})$. In the case of isomerization of 2,5-DHF, the reaction proceeds nearly to completion: the absorbances corresponding to the C−O stretches of $W(CO)_5(\eta^1\text{-2,5-DHF})$ return to within 3% of the baseline.

For reaction with 2,3-DHF, the same general features are observed: the absorbances corresponding to $W(CO)_5(CyH)$ disappear with a rate that depends on [DHF], followed by the disappearance of this product and appearance of a second product, the rate of which is independent of [DHF]. Figure 2 shows the time-dependent absorption at 1958 cm^{-1}, which happens to be near

---

[13] Schultz, R. H.; Bengali, A. A.; Tauber, M. J.; Weiller, B. H.; Wasserman, E. P.; Kyle, K. R.; Moore, C. B.; Bergman, R. G. *J. Am. Chem. Soc.* **1994**, *116*, 7369.

[14] Hermann, H.; Grevels, F.-W.; Henne, A.; Schaffner, K. *J. Phys. Chem.* **1982**, *86*, 5151.

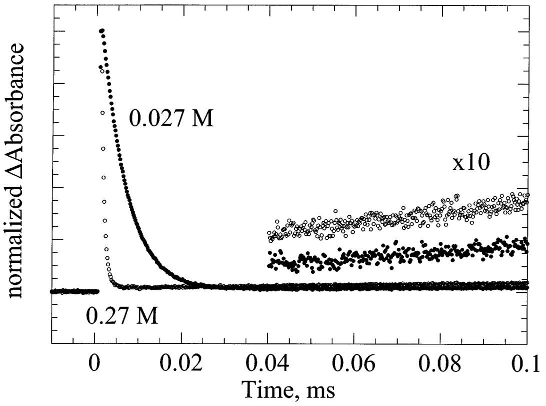

Figure 2. Time-dependent absorption at 1958 cm^{-1} following photolysis of a CyH solution of $W(CO)_6$ containing excess 2,3-DHF (●, [2,3-DHF] = 0.027 mol L^{-1}; ○, [2,3-DHF] = 0.27 mol L^{-1}). Shown are the concentration-dependent decay of the absorption due to $W(CO)_5(CyH)$ and the concentration-independent rise of the absorption due to $W(CO)_5(\eta^2\text{-DHF})$; the latter is also shown expanded by a factor of 10.

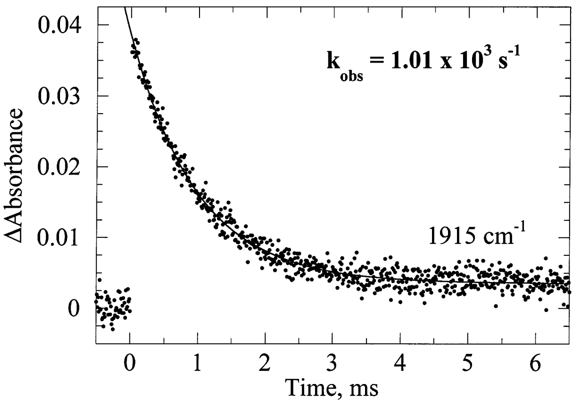

Figure 3. Time dependence ($T = 30$ °C) of the absorbance at 1915 cm^{-1} due to a C−O stretch of $W(CO)_5(\eta^1\text{-2,3-DHF})$. In this experiment, the initial concentration of $W(CO)_6$ was 8.8×10^{-4} mol L^{-1} and that of 2,3-DHF was 0.266 mol L^{-1}. The solid line is a single-exponential fit to the data with $k_{obs} = 1.01 \times 10^3$ s^{-1}.

an absorption peak both of $W(CO)_5(CyH)$ and of $W(CO)_5(\eta^2\text{-2,3-DHF})$, but not of $W(CO)_5(\eta^1\text{-2,3-DHF})$ (Table 1). As shown in Figure 2, the rate of decay of the $W(CO)_5(CyH)$ intermediate formed at the flash depends on [DHF], while the rate of formation of $W(CO)_5(\eta^2\text{-2,3-DHF})$ does not, consistent with bimolecular formation of the initial $W(CO)_5(\eta^1\text{-DHF})$ complex followed by intramolecular isomerization.

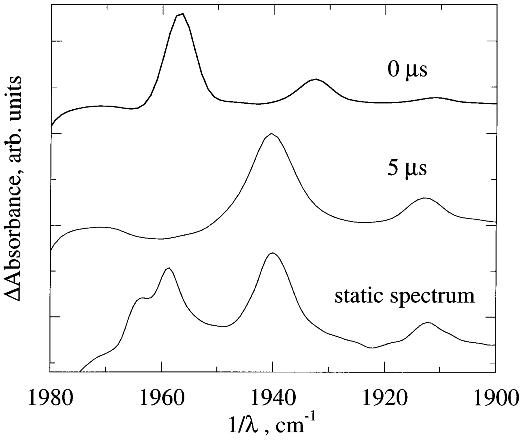

Figure 4. IR difference spectra following the photolysis of a CyH solution of $Cr(CO)_6$ in the presence of excess 2,5-DHF. Shown are the changes in absorbance (from top to bottom) immediately after the photolysis flash, 5 μs after the flash, and of a solution approximately 1 min after it was irradiated with ~250 laser shots.

Figure 3 shows the time dependence (measured at 30 °C) for the decay of one of the absorbances corresponding to $W(CO)_5(\eta^1\text{-2,3-DHF})$.[15] Two differences from the isomerization of the 2,5-DHF complex are immediately apparent. First, the isomerization of the 2,3-DHF complex is much faster than that of the 2,5-DHF complex; for example, at 30 °C, k_{obs} for isomerization of $W(CO)_5(\eta^1\text{-2,5-DHF})$ is ~4 s^{-1}, while k_{obs} for isomerization of $W(CO)_5(\eta^1\text{-2,3-DHF})$ is ~1000 s^{-1}. In addition, while reaction 1 proceeds essentially to completion for the 2,5-DHF complex, from Figure 3 it is clear that for the 2,3-DHF complex, even at the completion of the reaction, the absorbance has not returned to the baseline, indicating that a significant amount (in this case, ~10−20%) of the η^1 isomer remains even after the isomerization is complete.

$Cr(CO)_5(DHF)$ and $Mo(CO)_5(DHF)$. As is frequently the case for reactions of group 6 carbonyl complexes,[16] the kinetics of reaction 1 for M = Cr, Mo are more similar to each other than either is to the reaction for M = W. For this reason, they are treated together here. For both metals and for both isomers of DHF, k_{obs} does not depend on either [DHF] or [M]. Plots of the temperature dependences of k_{obs} are given as Figures S1 and S2 of the Supporting Information.

The longer term behavior of the Cr and Mo systems is also somewhat different from that of the W system. Shown in Figure 4 are typical IR spectra at different times following photolysis of $Cr(CO)_6$ in the presence of excess 2,5-DHF. The initially formed $Cr(CO)_5(CyH)$ complex reacts cleanly to form $Cr(CO)_5(\eta^1\text{-2,5-DHF})$. In contrast to the W + 2,5-DHF system shown in Figure 1, the absorbances of the two isomers of the $Cr(CO)_5(2,5\text{-DHF})$ complex are of similar magnitude even minutes after photolysis. For all of the Cr and Mo systems, A_∞/A_0, the ratio of the absorbance of a peak corresponding to the η^1 isomer at long times to the same absorbance immediately after formation of the η^1 complex from $M(CO)_5(CyH)$, is higher than that of the analogous W system.

Discussion

Deriving the Rate Constant for Isomerization. As noted above, for most of the systems studied here, while the absorbance corresponding to the η^1 isomer

---

[15] The transient was measured at 1915 cm^{-1}, even though, as shown in Table 1, the peak absorbance is at 1913 cm^{-1}. There are two reasons for this discrepancy. First of all, the peak locations were measured by S^2FTIR, while the kinetics were measured with our laser photolysis apparatus, and it appears that the calibrations of the two instruments are slightly different. Additionally, our IR laser produces a much stronger signal at 1915 cm^{-1} than it does at 1913 cm^{-1}, leading to a much better signal-to-noise ratio for the transient. As far as we have been able to tell, the peak shapes do not change significantly with time; therefore, the derived kinetics do not depend on how far from the peak maximum the measurements are made.

[16] Ziegler, T.; Tschinke, V.; Ursenbach, C. *J. Am. Chem. Soc.* **1987**, *109*, 4825 and references therein.

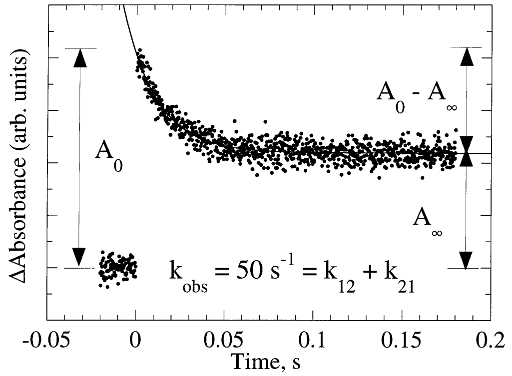

Figure 5. Illustration of the derivation of K_{eq} and k_{12}. Shown is the normalized time-dependent absorbance of Mo(CO)$_5$(η^1-2,5-DHF) (monitored at 1915 cm^{-1}) following photolysis of a solution containing 6.7×10^{-4} mol L^{-1} Mo(CO)$_6$ and 0.019 mol L^{-1} 2,5-DHF. The solid line is a least-squares single-exponential fit to the data with $k_{obs} = 50$ s^{-1}. Also indicated are the normalized A_0 and A_∞, the initial and final ΔAbsorbance at that wavelength.

eventually ceases to change with time, the absorbance itself does not return to baseline, indicating that even at the completion of the reaction, some of the η^1 isomer remains in solution. We believe that the most likely explanation for this behavior is that the isomerization is reversible, as shown in reaction 2. Since at the

$$\mathrm{M(CO)_5(CyH)} \xrightarrow[\mathrm{[DHF]}]{k_a} \mathrm{M(CO)_5(\eta^1\text{-}DHF)} \underset{k_{21}}{\overset{k_{12}}{\rightleftharpoons}} \mathrm{M(CO)_5(\eta^2\text{-}DHF)} \quad (2)$$

initiation of the reaction [M(CO)$_5$(η^2-DHF)] = 0, k_{obs}, the observed first-order rate constant for the decay of the absorbance of M(CO)$_5$(η^1-DHF), is equal to the sum of the forward and reverse rate constants for isomerization (k_{12} and k_{21}, respectively).[17] We can obtain the forward isomerization rate k_{12} from the experimental data if we assume that reactions of M(CO)$_5$(DHF) other than isomerization are much slower than the isomerization itself. Since M(CO)$_5$(DHF) is much more stable than M(CO)$_5$(CyH), we treat the formation of M(CO)$_5$(η^1-DHF) as irreversible. On the basis of these assumptions, we can treat the system after the absorption of the η^1 isomer ceases to change with time as an equilibrium and define the equilibrium constant K_{eq} by eq 3,

$$K_{eq} = \frac{[\mathrm{M(CO)_5(\eta^2\text{-}DHF)}]}{[\mathrm{M(CO)_5(\eta^1\text{-}DHF)}]} = \frac{A_0 - A_\infty}{A_\infty} = \frac{k_{12}}{k_{21}} \quad (3)$$

where A = the absorbance due to the η^1 isomer. Since the reaction is intramolecular, $(A_0 - A_\infty) \propto$ [M(CO)$_5$(η^2-DHF)]$_\infty$. Thus, as illustrated in Figure 5, we can calculate K_{eq} from A_0 and A_∞ and k$_{12}$ from eq 4.

$$k_{12} = \frac{k_{obs}}{1 + \dfrac{1}{K_{eq}}} \quad (4)$$

Tables of the temperature-dependent values of k_{obs} and A_∞/A_0 and of the values of k_{12} and K_{eq} derived from eqs 3 and 4 are given in the Supporting Information.[18]

Reaction at Low [DHF]. As was mentioned above, as a check that reaction 1 proceeds intramolecularly, we performed independent kinetic measurements with varying [DHF] (by a factor of at least 10) and observed that k_{obs} is independent of [DHF]. In some cases, however, we observed an apparent dependence of A_∞/A_0 on [DHF]. For example, in the isomerization of Mo(CO)$_5$(2,3-DHF), measurements made at [DHF] = 0.21 mol L^{-1} and 2.7 mol L^{-1} are the same to within experimental error. When [DHF] = 0.011 mol L^{-1}, however, A_∞/A_0 seems to be significantly higher (see Figure S3 of the Supporting Information). Since K_{eq} and k_{12} are determined from the experimentally determined value of A_∞/A_0, a dependence of A_∞/A_0 on [DHF] at low but not at high concentrations might indicate that we are observing some kind of process that leads to kinetic saturation at high [DHF].

We find this explanation unlikely, however. In the first place, it is difficult to imagine a reasonable kinetic scheme that would affect A_∞/A_0 but not k_{obs}. In fact, terms containing [DHF] cancel both from the rate expression for k_{obs} and from the expression for "K_{eq}" (i.e., [M(CO)$_5$(η^2-DHF)]/[M(CO)$_5$(η^1-DHF)]) for the simplest kinetic schemes that involve free DHF in the isomerization, such as a competing dissociative pathway or isomerization that requires interaction with a second molecule of DHF. We also considered more complicated kinetic schemes: for example, inclusion of dissociation of M(CO)$_5$(DHF) to nonreactive products or explicit inclusion of the solvent as a reactant. For these kinetic schemes, for which analytic solutions are either impossible or unduly complicated, we attempted to model the kinetics using Richardson's "KinFit" program.[19] We were not able to replicate the observed kinetics using reasonable values for the various rate constants.

Rather, we believe that the correct explanation is that this apparent [DHF] dependence of A_∞/A_0 is an experimental artifact. As mentioned above, the kinetic measurements from which we derive K_{eq} and k_{12} are made by measuring the time-dependent absorbance of the low-energy A$_1$ band of M(CO)$_5$(η^1-DHF) at ~1915 cm^{-1}. This frequency was chosen because it does not overlap with an absorption of the η^2 isomer. It does, however, coincide or nearly coincide with an absorption of the previously observed[14] M(CO)$_5$(H$_2$O) complex. Although the CyH solvent was distilled from Na/benzophenone, some traces of water may remain in the solution or enter it during its preparation. At the lowest [DHF] concentrations, even these traces of water ($<10^{-3}$ mol L^{-1}) can compete with DHF for the M(CO)$_5$(CyH) intermediate,[20] since the second-order rate constant for formation of M(CO)$_5$(H$_2$O) is much higher than that for formation of M(CO)$_5$(DHF).[3,14] Under our experimental conditions,

---

[17] Steinfeld, J. I.; Francisco, J. S.; Hase, W. L. *Chemical Kinetics and Dynamics*; Prentice Hall: Englewood Cliffs, NJ, 1989; Chapter 2.

[18] While an analogous calculation could be done to determine k_{21}, and K_{eq} then could be calculated from the ratio of the two rate constants, we chose to calculate K_{eq}, since the actual measurement we make is of the relative amounts of the two isomers rather than of the relative rate constants of the forward and reverse reactions. Not surprisingly, calculation of k_{21} rather than K_{eq} gives equilibrium parameters (from the relative forward and reverse rate constants and activation barriers) that are entirely consistent with those given in Table 2.

[19] Richardson, D. E. Kinfit32 version 0.9e for Windows; available for download from http://www.chem.ufl.edu/~der/chm6621.htm.

[20] Another possibility is that traces of acetone, which is used in cleaning the volumetric flasks in which the solutions are prepared, enters the solution if the volumetric flask is incompletely dried, and the M(CO)$_5$(acetone) complex is formed.

Table 2. Activation and Equilibrium Parameters for Reaction 1[a]

syst	$\Delta H^\ddagger$, kcal/mol^{-1}	$\Delta S^\ddagger$, eu	$\Delta H°$, kcal/mol^{-1}	$\Delta S°$, eu
Cr/2,5-DHF	17.1 ± 0.3	4.2 ± 1.1	−2.5 ± 0.5	−8.8 ± 1.4
Mo/2,5-DHF	14.8 ± 0.3	−0.6 ± 1.4	−2.1 ± 0.2	−6.9 ± 0.6
W/2,5-DHF[b]	17.3 ± 0.4	1.0 ± 1.1	*c*	*c*
Cr/2,3-DHF	13.7 ± 0.3	4.0 ± 1.1	−2.4 ± 0.5	−4.5 ± 1.5
Mo/2,3-DHF	11.2 ± 0.4	−2.2 ± 2.1	−1.2 ± 0.6	−1.3 ± 2.1
W/2,3-DHF	13.3 ± 0.2	−1.2 ± 0.9	−0.9 ± 0.4	1.2 ± 1.3

[a] k_{12} and K_{eq} were determined from eqs 3 and 4; reported uncertainties are 1σ in the parameters used to fit the temperature dependences of ln(k_{12}/T) and ln(K_{eq}). [b] Reference 1. [c] A_∞ too small for accurate determination of K_{eq}; see text.

there would be no unambiguous evidence of the presence of $M(CO)_5(H_2O)$ in the kinetic traces for reaction 1, since $M(CO)_5(H_2O)$ and $M(CO)_5(\eta^1\text{-DHF})$ are formed simultaneously, and both are stable on the time scale of the isomerization. Thus, the net result of the presence of a contaminant such as H_2O on the *experimentally* observed kinetics of reaction 1 would be to yield a spuriously low value of K_{eq} but no change in k_{obs}.[21] This hypothesis also explains the results shown in Figure 2: although the *rate* of formation of the η^2 isomer is independent of [DHF], the *amount* formed relative to the amount of $W(CO)_5(CyH)$ intially present is higher at the higher [DHF] concentration; at low [DHF], a greater proportion of the $W(CO)_5(CyH)$ reacts to form $W(CO)_5(H_2O)$ rather than $W(CO)_5(DHF)$. Not only will the amount of H_2O impurity present probably vary from run to run, but also, to maximize the signal-to-noise ratio, we run the monochromator at a resolution only sufficient to separate the diode laser modes. Thus, absolute quantitation of this effect would be quite difficult and was not attempted.

As a result of these considerations, the derived parameters given below are all taken from experimental runs at [DHF] > 0.2 mol L^{-1}, high enough that A_∞/A_0 is independent (to within experimental error) of [DHF]. We note, however, that even if the preceding analysis is entirely wrong and the only correct results are those measured at *low* [DHF], none of the derived activation parameters reported below would change by as much as 10%. The error introduced in this worst case is small due to the small *absolute* differences in and weak temperature dependence of A_∞/A_0.

Trends in k_{12}. Eyring activation parameters for reaction 1, as determined from the temperature dependence of k_{12}, are given in Table 2. Eyring analyses of the temperature dependences of k_{12} are shown pictorially for isomerization of $M(CO)_5(2,5\text{-DHF})$ in Figure 6. A similar plot for isomerization of $M(CO)_5(2,3\text{-DHF})$ is given as Figure S4 of the Supporting Information. As a specific illustration of the relative reactivities of the six systems, 300 K values for k_{12} and K_{eq}, calculated from these analyses, are given in Table 3.

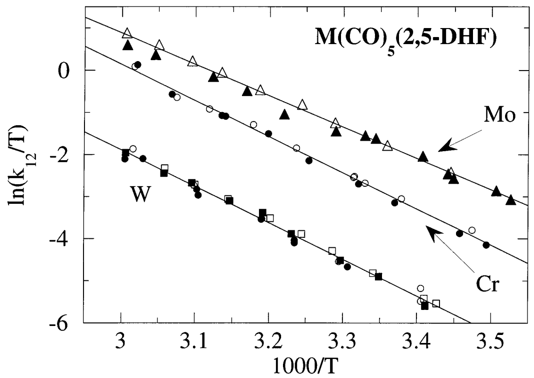

Figure 6. Eyring analysis of k_{12}, derived as described in the text, for the linkage isomerization of $M(CO)_5(2,5\text{-DHF})$. Different symbols represent different DHF concentrations. The solid lines are weighted least-squares linear fits to the data.

Table 3. Calculated Values of k_{12} and K_{eq} for Reaction 1 at 300 K[a]

syst	k_{12}, s^{-1}	K_{eq}	syst	k_{12}, s^{-1}	K_{eq}
Cr/2,5-DHF	19	0.9	Cr/2,3-DHF	5.3×10^3	5.7
Mo/2,5-DHF	60	1.0	Mo/2,3-DHF	1.3×10^4	4.3
W/2,5-DHF	~2.5	>30	W/2,3-DHF	7.2×10^2	8.8

[a] Calculated from fits to the temperature dependences of k_{12} (eq 4) and K_{eq} (eq 3).

For all six systems studied here, the values of $\Delta H^\ddagger$ for reaction 1 are significantly higher than those for ligand substitution at $M(CO)_5$(alkane) complexes[3,12,22] but considerably lower than those for thermal ligand substitution at $M(CO)_6$.[16] The activation parameters measured for reaction 1 are very similar to those determined by Jeong and Holwerda[7] for the linkage isomerization of $Pd(PPh_3)_2$(chloraniline) from σ,σ-bound to π,π-bound; for the Pd system, $\Delta H^\ddagger = 17.1$ kcal mol^{-1} and $\Delta S^\ddagger = -6$ eu.

In the present systems, over the temperature range studied, k_{12} for complexes with the same isomer of DHF follows the order Mo > Cr > W, typical for reactions of carbonyl complexes of group 6 metals.[16] A more detailed comparison (Table 2) shows that $Mo(CO)_5(\eta^1\text{-DHF})$ isomerizes more rapidly than the analogous W complex, primarily due to differences in $\Delta H^\ddagger$; $\Delta S^\ddagger \approx 0$ for reaction 1 both for Mo and for W.[23] On the other hand, the more rapid reaction of Cr relative to that of W appears to be due to higher $\Delta S^\ddagger$ values in the Cr complexes. These trends in $\Delta H^\ddagger$ (Mo < Cr ≈ W) and $\Delta S^\ddagger$ (Mo ≈ W < Cr) in reactions of group 6 carbonyl complexes have previously been observed in ligand substitution reactions of $M(CO)_6$[16,24] and of photolytically generated $M(CO)_5$(alkane) complexes[3,12,22,25] and have been attributed to electronic[16] and steric[25] differences in the metal−ligand bonds.

The trend in $\Delta S^\ddagger$ in reaction 1 may also indicate that isomerization of $Cr(CO)_5(DHF)$ goes through a more

---

[21] If H_2O were being added with incompletely dried DHF, we would expect A_∞ to rise with increasing [DHF] rather than to fall, as is observed.

[22] (a) Dobson, G. R.; Spradling, M. D. *Inorg. Chem.* **1990**, *29*, 880. (b) Dobson, G. R.; Asali, K. J.; Cate, C. D.; Cate, C. W. *Inorg. Chem.* **1991**, *30*, 4417. (c) Dobson, G. R.; Zhang, S. *J. Coord. Chem.* **1999**, *47*, 409.

[23] In the case of associative ligand substitution at $W(CO)_5(CyH)$, $\Delta S^\ddagger$ is significantly negative.[3,12]

[24] (a) Werner, H.; Prinz, R. *Chem. Ber.* **1960**, *99*, 3582. (b) Graham, J. R.; Angelici, R. J. *Inorg. Chem.* **1967**, *6*, 2082. (c) Covey, W. D.; Brown, T. L. *Inorg. Chem.* **1973**, *12*, 2820. (d) Kirtley, S. W. In *Comprehensive Organometallic Chemistry*; Wilkinson, G., Stone, F. G. A., Abel, E. W., Eds.; Pergamon: New York, 1982; Vol. 3, Chapter 26.1. (e) Darensbourg, D. J. *Adv. Organomet. Chem.* **1982**, *21*, 113.

[25] (a) Awad, H. H.; Dobson, C. B.; Dobson, G. R.; Leipholdt, J. G.; Schneider, K.; van Eldik, R.; Wood, H. W. *Inorg. Chem.* **1989**, *28*, 1654. (b) Dobson, G. R.; van Eldik, R. *J. Organomet. Chem.* **1990**, *397*, 279. (c) Wieland, S.; van Eldik, R. *Organometallics* **1991**, *10*, 3110. (d) Zhang, S.; Bajaj, H. C.; Zang, V.; Dobson, G. R.; van Eldik, R. *Organometallics* **1992**, *11*, 3901.

dissociative transition state than the other two metals. A trend from dissociative (Cr) to associative (W) behavior has also been noted in the ligand substitution reactions of group 6 transient species.[25] Although reaction 1 may go through a looser transition state when M = Cr than when M = Mo or W, in all six cases studied here, the low values of $\Delta S^‡$ (Arrhenius preexponential factors of $\sim 10^{13}-10^{14}$) are consistent with the intramolecular isomerization mechanism suggested by the independence of k_{12} from [DHF].

For a given metal, reaction 1 invariably proceeds much faster (at room temperature, by a factor of on the order of 10^2) for isomerization of $M(CO)_5$(2,3-DHF) than for $M(CO)_5$(2,5-DHF). The difference in reactivity primarily reflects differences in $\Delta H^‡$ values, which in all cases are ~3 kcal/mol lower in the former reaction; for a given metal, $\Delta S^‡$ is nearly independent of which isomer of DHF is bound to the metal. The most intuitive explanation for the difference in the reactivities of 2,5- and 2,3-DHF is that, in the latter, the double bond is closer to the oxygen atom, requiring less rearrangement to reach the transition state.

Additional evidence supporting this conjecture comes from a calculation of frontier molecular orbitals (FMOs) of the two isomers of DHF. We used Gaussian 98[26] to perform DFT calculations (B3LYP level, CEP-31G* basis set) of the structures and molecular orbitals of 2,3-DHF and 2,5-DHF. The calculated geometries of the DHF isomers are in good agreement with experiment[27] and other recent calculations.[28] According to our calculations, the primary components of both the HOMO and the LUMO of 2,3-DHF are the $C(p_z)$ orbitals that form the double bond and the $O(p_z)$ orbital. In the case of 2,5-DHF, the HOMO again comprises primarily contributions from the $C(p_z)$ orbitals of the double bond and from the $O(p_z)$ orbital, while the LUMO is essentially the π^* orbital of the double bond. Since for 2,3-DHF the frontier orbitals have contributions from three consecutive atoms along the ring, the isomerization can be expected to proceed via a "conducted tour" mechanism,[29] which is not available as a low-energy pathway for the isomerization of the 2,5-DHF complexes, for which the metal atom must necessarily travel across the face of the ring.[30,31] FMO theory has previously been used to explain peculiarities of the kinetics of enol ethers (of which 2,3-DHF is an example), primarily in the context of Diels–Alder and similar pericyclic reactions.[32]

These differences in $\Delta H^‡$ for reactions of the two isomers of DHF may, however, reflect electronic rather than geometrical effects. In our studies of ligand substitution at $W(CO)_5$(CyH),[3,12,33] we found that as the incoming ligand becomes more strongly electron-donating, $\Delta H^‡$ for the reaction decreases (except in cases where steric interference slows the reaction). We explained this observation in terms of an associative substitution mechanism, in which a more electron-donating ligand can better stabilize the transition state as the cyclohexane molecule leaves, while an electron-withdrawing ligand is less capable of such stabilization. Table 1 gives the C–O stretching force constants for the various $M(CO)_5$(DHF) complexes, and from these values, it is clear that in all cases η^2-2,5-DHF is more strongly electron-withdrawing than η^2-2,3-DHF. Apparently, the same considerations that determine the activation barrier in the case of ligand substitution apply to reaction 1 as well. Indeed, we can think of reaction 1 as an "intramolecular associative ligand substitution" reaction in which the coordinated oxygen atom is replaced by a double bond, as seen in the trends in k_{12} both as a function of the metal and as a function of the isomer of DHF being studied. Unlike the case of ligand substitution at $M(CO)_5$(solvent), however, in reaction 1, the reverse reaction generally proceeds at a rate comparable to that of the forward reaction.

Trends in K_{eq}. Analyses of the derived equilibrium constants K_{eq} are summarized in Tables 2 and 3. A van't Hoff plot for M = Cr is shown in Figure 7; similar plots for M = Mo, W are given as Figures S5 and S6 of the Supporting Information. As is clear from the temperature dependence of K_{eq} shown in the figures, in all cases, reaction 1 is exothermic, and the enthalpy and energy differences between the two linkage isomers are both much smaller than those of the barrier that separates them. We can compare these results to those obtained by Gladysz and co-workers[8] in their studies of the equilibrium between the $\eta^1(\sigma) \rightleftharpoons \eta^2(\pi)$ linkage isomers of a number of [Re]–aldehyde complexes. They reported values of $\Delta H°$ similar to those we derive here for reaction 1 and values of $\Delta S°$ similar to those we have determined for the isomerizations involving 2,5-DHF. Gladysz and co-workers did not report activation parameters for the isomerizations that they studied.

---

[26] Frisch, M. J.; Trucks, G. W.; Schlegel, H. B.; Scuseria, G. E.; Robb, M. A.; Cheeseman, J. R.; Zakrzewski, V. G.; Montgomery, J. A.; Stratmann, R. E.; Burant, J. C.; Dapprich, S.; Milam, J. M.; Daniels, A. D.; Kudin, K. N.; Strain, M. C.; Farkas, O.; Tomasi, J.; Barone, V.; Cossi, M.; Cammi, R.; Mennucci, B.; Pomelli, C.; Adamo, C.; Clifford, S.; Ochterski, J.; Petersson, G. A.; Ayala, P. Y.; Cui, Q.; Morokuma, K.; Malick, D. K.; Rabuck, A. D.; Raghavachari, K.; Foresman, J. B.; Cioslowski, J.; Ortiz, J. V.; Stefanov, B. B.; Liu, G.; Liashenko, A.; Piskorz, P.; Komaromi, I.; Gomperts, R.; Martin, R. L.; Fox, D. J.; Keith, T.; Al-Laham, M. A.; Peng, C. Y.; Nanayakkara, A.; Gonzalez, C.; Challacombe, M.; Gill, P. M. W.; Johnson, B. G.; Chen, W.; Wong, M. W.; Andres, J. L.; Head-Gordon, M.; Replogle, E. S.; Pople, J. A. *Gaussian 98*, revision A.7; Gaussian, Inc.: Pittsburgh, 1998.

[27] (a) Tamagawa, K.; Hilderbrandt, R. L. *J. Am. Chem. Soc.* **1984**, *106*, 20. (b) Cervellati, R.; Degli Esposti, A.; Lister, D. G.; Lopez, J. C.; Alonso, J. L. *J. Mol. Struct.* **1986**, *147*, 255.

[28] (a) Autrey, D.; Laane, J. *J. Phys. Chem. A* **2001**, *105*, 6894. (b) Dubnikova, F.; Lifshitz, A. *Int. J. Chem. Kinet.* **2001**, *33*, 687.

[29] (a) Cram, D. J.; Gosser, L. *J. Am. Chem. Soc.* **1964**, *86*, 2950. (b) Cram, D. J.; Willey, F.; Fischer, H. P.; Scott, D. A. *J. Am. Chem. Soc.* **1964**, *86*, 5370. Our calculated structures for $M(CO)_5(\eta^2$-2,3-DHF)[31] indicate that the isomerization can proceed along a single face of the DHF ring.

[30] For some examples of applications of frontier MO theory to reactions of organometallic complexes, see ref 16 and: (a) Silvestre, J. *New J. Chem.* **1988**, *12*, 9. (b) Manna, J.; Gilbert, T. M.; Dallinger, R. F.; Geib, S. J.; Hopkins, M. D. *J. Am. Chem. Soc.* **1992**, *114*, 5870. (c) Bueker, H. H.; Maitre, P.; Ohanessian, G. *J. Phys. Chem. A* **1997**, *101*, 3966. (d) Wagner, N. L.; Kloss, J. M.; Murphy, K. L.; Bennett, D. W. *J. Chem. Inf. Comput. Sci.* **2001**, *41*, 50.

[31] We are currently extending the above-mentioned DFT calculations to include the complexes themselves (Shagal, A.; Aped, P.; Schultz, R. H. work in progress). These calculations indicate that while the simple assumptions of FMO theory (Fukui, K.; Fujimoto, H. *Bull. Chem. Soc. Jpn.* **1969**, *42*, 3399) cannot entirely explain the reactivity patterns observed in the present experiments, there are some additional interesting correlations: for example, for a given metal, the HOMO–LUMO gap in $M(CO)_5(\eta^1$-DHF) is always smaller for the complex containing 2,3-DHF.

[32] (a) Houk, K. N. *J. Am. Chem. Soc.* **1973**, *95*, 4092. (b) Wong, S. S.; Paddon-Row, M. N.; Li, Y.; Houk, K. S. *J. Am. Chem. Soc.* **1990**, *112*, 8679. (c) Yoshioka, Y.; Yamada, S.; Kawakami, T.; Nishino, M.; Yamaguchi, K.; Saito, I. *Bull. Chem. Soc. Jpn.* **1996**, *69*, 2683. (d) Pugnaud, S.; Masure, D.; Halle, J.-C.; Chaquin, P. *J. Org. Chem.* **1997**, *62*, 8687. (e) Bonnarme, V.; Bachmann, C.; Cousson, A.; Mondon, M.; Gesson, J.-P. *Tetrahedron* **1999**, *55*, 433.

[33] Krishnan, R.; Schultz, R. H. *Organometallics* **2001**, *20*, 3314.

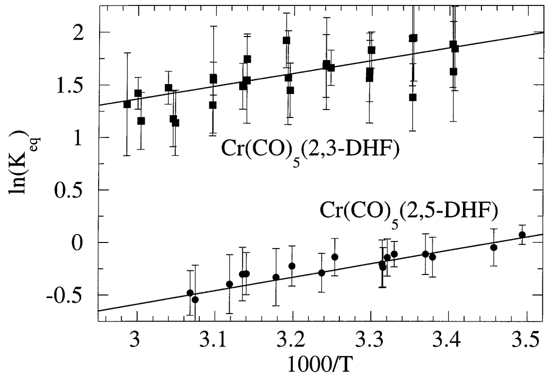

Figure 7. van't Hoff plot for linkage isomerization of $Cr(CO)_5$(2,5-DHF) (●) and $Cr(CO)_5$(2,3-DHF) (■). The graph shows ln K_{eq}, derived by using eqs 3 and 4, as a function of 1000/T. The solid lines are weighted least-squares linear fits to the data; error bars represent 1σ uncertainties in the derived values of ln K_{eq}.

Returning to the present work, the relative hardness of the metal also plays a significant role in the thermodynamics of the isomerization equilibrium. As shown in Table 3, at 300 K, for isomerization of $M(CO)_5$(2,5-DHF), the equilibrium mixture for M = Cr, Mo is about 1:1, while for M = W, the η^2 isomer is favored by a factor of at least 30. This is consistent with the relative softness of W, which prefers to bind to polarizable π-acceptor ligands in preference to hard σ-donors such as ethers. For the harder metals Cr and Mo, the preference for binding to the double bond is much less strong. These results are analogous to those observed by Angelici and co-workers[34] for the equilibrium between the η^1(S)- and η^2(C=C)-bound isomers of (C_5R_5)-$Re(CO)_2$(DBT) (DBT = benzo[*b*]thiophene): when R = CH_3, the equilibrium favors the η^2 form more than when R = H. Interestingly, only η^1 binding was observed for $M(CO)_5$(DBT) (M = Cr, W)[35] and $W(CO)_5$(DHT) (DHT = 2,5-, 2,3-dihydrothiophene).[36]

For the $M(CO)_5$(2,3-DHF) complexes, at 300 K, K_{eq} is approximately 4−5 for M = Cr, Mo. Not surprisingly in light of the above discussion, it is somewhat higher (~9) for M = W. More interesting is the observation that for M = Cr, Mo, the equilibrium constant is higher for $M(CO)_5$(2,3-DHF) than it is for $M(CO)_5$(2,5-DHF), while for M = W, the reverse is true. Again, we can explain this trend qualitatively in terms of the different properties of the two DHF ligands and the relative hardness of the three metals. The softest metal, W, has the greatest thermodynamic preference for the softer ligand. In addition, W, which is the most π-basic of the three metals, has the strongest thermodynamic preference for the more electron-withdrawing double bond. Note that this thermodynamic preference, which reflects the relative stabilities of the isomers, is opposed to the kinetic preference, in which a more strongly electron-withdrawing alkene is less able to stabilize the transition state for the isomerization and reacts more slowly.

In the case of Cr and Mo, however, the thermodynamic preferences (K_{eq} is larger for 2,3-DHF) do match the relative kinetics. Presumably, these less basic metals bind less strongly to the less electron-withdrawing double bond; indeed, since 2,3-DHF is an enol ether, there is a resonance structure that places negative charge on C3 of the ring. We have previously discussed the effects of this structural feature in the context of its effects on the kinetics of ligand exchange at $W(CO)_5$-(CyH);[3] here, we can see the thermodynamic effects as well when we contrast the behavior of W with that of Cr and Mo.

Summary and Conclusions

In this work, linkage isomerization reactions of $M(CO)_5$(DHF) (M = Cr, Mo, W; DHF = 2,3-, 2,5-DHF) were studied by time-resolved infrared absorption spectroscopy. In all cases, DHF reacts with a photolytically generated $M(CO)_5$(solvent) complex to form as the sole kinetic product $M(CO)_5(\eta^1$-DHF), bound through the ligand's oxygen atom. The kinetic product then undergoes an intramolecular isomerization to yield an equilibrium mixture of the η^1 and η^2 forms, the latter bound through the ligand's double bond. We have shown that TRIR is an ideal method not only for studying the kinetics of the approach to equilibrium but also for studying the equilibrium subsequently established. We have found, however, that in order to obtain accurate measurements of the $\eta^1 \rightleftharpoons \eta^2$ equilibrium, the experimental conditions must be chosen to minimize interference from complexes such as $M(CO)_5(H_2O)$ that have IR absorption spectra similar to that of $M(CO)_5(\eta^1$-DHF).

The activation enthalpies for the linkage isomerization reaction are generally ~10−15 kcal mol^{-1}, with near-zero activation entropies. Trends in the kinetics of the linkage isomerization reactions bear similarities to those of the ligand substitution reactions of $M(CO)_6$ and $M(CO)_5$(L): the room-temperature isomerization rate for a given ligand follows the order Mo > Cr > W, and formation of the η^2 isomer is faster for the less electron-withdrawing alkene, 2,3-DHF.

For each complex, the energy difference between the two isomers is much less than the barrier that separates them. Trends in the equilibrium parameters can be understood in terms of the properties of the metals. For example, W shows a greater preference for the η^2 form than Cr and Mo do. In addition, the equilibrium constant for the isomerization, $[\eta^2]/[\eta^1]$, follows the order 2,5-DHF > 2,3-DHF for W, while the opposite is true for Cr and Mo. Since W is a "softer" π-base than the other two metals, it shows a greater preference for the softer ligand.

Further studies are currently underway with substituted dihydrofurans and dihydropyrans to see if the steric and electronic effects that have been observed in the ligand exchange reactions of $M(CO)_5$(solvent) continue to appear in intramolecular linkage isomerization reactions of $M(CO)_5$(L) complexes.

Acknowledgment. This work was supported by the Israel Science Foundation, founded by the Israel Academy of Arts and Sciences, and by the Bar-Ilan University Research Authority. R.H.S. thanks Dr. Ashfaq Bengali (Dickinson College) for useful discussions.

---

(34) Choi, M.-G.; Angelici, R. J. *Organometallics* **1992**, *11*, 3328.

(35) Reynolds, M. A.; Guzei, I. A.; Logsdon, B. C.; Thomas, L. M.; Jacobson, R. A.; Angelici, R. J. *Organometallics* **1999**, *18*, 4075.

(36) (a) Sauer, N. N.; Angelici, R. J. *Inorg. Chem.* **1987**, *26*, 2160. (b) Choi, M.-G.; Daniels, L. M.; Angelici, R. J. *Inorg. Chem.* **1991**, *30*, 3647.

Supporting Information Available: Figures S1–S6, showing the temperature dependences of k_{obs} for reaction 1, the [DHF] concentration dependence of K_{eq} for isomerization of Mo(CO)$_5$(2,3-DHF), Eyring plots for the isomerization of M(CO)$_5$(2,3-DHF) and van't Hoff plots for isomerization of W(CO)$_5$(2,3-DHF) and Mo(CO)$_5$(DHF), and tables of experimental first-order rate constants (k_{obs}), A_∞/A_0, and derived η^2/η^1 isomer ratios (K_{eq}) and isomerization rate constants (k_{12}) for reaction 1. This information is available free of charge via the Internet at http://pubs.acs.org.

OM020084F